Infrared spectroscopy of the cluster ions $H_3^+ \cdot (H_2)_n$

M. Okumura,[a] L. I. Yeh, and Y. T. Lee
Materials and Chemical Sciences Division, Lawrence Berkeley Laboratory and Department of Chemistry, University of California, Berkeley, California 94720

(Received 26 August 1987; accepted 16 September 1987)

The vibrational spectra of the clusters $H_3^+ (H_2)_n$ were observed near 4000 cm^{-1} by vibrational predissociation spectroscopy. Spectra of mass-selected clusters were obtained by trapping the ions in a radio frequency ion trap, exciting vibrational transitions of the cluster ions to predissociating levels, and detecting the fragment ions with a mass spectrometer. Low resolution bands of the solvent H_2 stretches were observed for the clusters of one to six H_2 coordinated to an H_3^+ ion. The red shift of these vibrations relative to the monomer H_2 frequency supported the model of H_9^+ as an H_3^+ with a complete inner solvation shell of three H_2, one bound to each corner of the ion. Two additional bands of H_5^+ were observed, one assigned as the H_3^+ symmetric stretch, and the other as a combination or overtone band. High-resolution scans (0.5 and 0.08 cm^{-1}) of H_n^+, $n = 5$, 7, and 9 yielded no observable rotational structure, a result of either spectral congestion or rapid cluster dissociation. The band contour of the H_5^+ band changed upon cooling the internal degrees of freedom, but the peaks remained featureless. The observed frequencies of H_7^+ and H_9^+ agreed well with *ab initio* predictions, but those of H_5^+ did not. This deviation is discussed in terms of the large expected anharmonicity of the proton bound dimer H_5^+.

I. INTRODUCTION

Ionic clusters such as $H_3O^+ \cdot (H_2O)$ are important species in the stratosphere,[1] where molecules readily nucleate about ions as a result of the long-range attractive forces that dominate ion–molecule interactions. Such weakly bound molecular cluster ions have thus attracted much attention.[2] Cluster ions have also been studied to shed light on ion–solvent interactions in liquids.[3] The energetics, kinetics, and dynamics of cluster association and dissociation have been investigated by a variety of experimental techniques, but questions about the structure and vibrational motions of these ions remain largely unanswered.[2,4] Traditionally, these problems have been addressed by gas phase spectroscopy. Although the spectroscopy of molecular ions has developed rapidly in the past decade,[5,6] the spectroscopy of cluster ions has proven to be very difficult.

While only a handful of spectroscopic investigations of cluster ions have been done, several promising developments have been reported in the past year. In the earliest studies, Schwarz observed low resolution infrared absorption spectra of the $H_3O^+ \cdot (H_2O)_m$ and $NH_4^+ \cdot (NH_3)_m$ clusters created in the pulsed radiolysis of water (and ammonia) vapor. More recently, Kennedy and Miller[7] have obtained laser induced fluorescence spectra of the clusters $C_6F_6^+ \cdot He$, and from observation of vibronic transitions involving the intermolecular vibrations, have estimated the geometry and force field for this cluster. Smalley and co-workers[8] have reported electronic spectra of Nb_2^+ and Ni_2^+ using a two-photon dissociation scheme to probe the bound intermediate state. Several groups are studying cluster anions by photoelectron spectroscopy.[9–11] An important advance has been made by Bogey *et al.*[12] who have observed the microwave spectra of $Ar \cdot H_3^+$ and $Ar \cdot D_3^+$ in a glow discharge, the first high-resolution spectra of weakly bound ions. We have recently reported preliminary results on the infrared spectroscopy of cluster ions using vibrational predissociation spectroscopy.[13,14] In this paper, we describe our experiments on the hydrogen cluster ions $H_3^+ \cdot (H_2)_n$.

The hydrogen cluster ions are the simplest ionic molecular complexes. The structure of these clusters has generally been described as H_2 molecules surrounding the H_3^+ ion, $H_3^+ \cdot (H_2)_n$. H_3^+ itself is a dominant ion in many hydrogen discharges[15] and plasmas, and is expected to be abundant in the interstellar medium. The proton affinity of H_2 is 101 kcal/mol,[16] so the H_3^+ ion is strongly bound. The H_5^+ ion was first positively identified by Dawson and Tickner in 1962[17] by mass spectrometry. Larger odd mass clusters were subsequently observed by Buchheit and Henkes in mass spectra[18] and by Clampitt and Gowland using low energy electron bombardment of solid hydrogen.[19] Later workers have observed odd mass hydrogen clusters in various size distributions from ionization and collisional fragmentation studies.[20–24] Kirchner and Bowers have studied the dynamics of metastable H_5^+ fragmentation.[25] High-pressure mass spectrometry and drift tube experiments have yielded the enthalpy and entropy of association for the ionic hydrogen clusters,[26–32] and found that they are bound by less than 10 kcal/mol. Although there is some disagreement concerning the H_5^+ dissociation enthalpy, the most recent measurements[31,32] give $\Delta H^0_{300} = 5.8$ and 6.6 kcal/mol for $H_5^+ \rightleftharpoons H_3^+ + H_2$ and $\Delta H^0_{110} = 3.1$ kcal/mol for $H_7^+ \rightleftharpoons H_5^+ + H_2$. The only previous reports of hydrogen cluster ion spectra have been charge-induced spectra observed in radiation-damaged solid hydrogen isotopes (D_2 and T_2).[33–35] Although the observed peaks have been attributed in part to

[a] Current address: Chemistry Department, The University of Chicago, Chicago, IL 60637.

cluster ion formation, no definitive assignment has been made.

Their small size makes these clusters ideal for accurate computational study, and there have been many *ab initio* calculations. Theorists have also found that these clusters are very weakly bound, and require fairly large basis sets and correlation for converging results.[36–47] Table I contains a compilation of the experimental results and a selection of *ab initio* calculations for the H_n^+ dissociation energies. In the best calculation on H_5^+ to date,[47] Yamaguchi *et al.* predict $D_0 = 5.45$ kcal/mol, and inclusion of the thermal contribution (using calculated vibrational frequencies to estimate the vibrational partition function) yields $\Delta H^0_{300} = 6.5$ to 7 kcal/ mol, in good agreement with the most recent experimental values. The *ab initio* studies all conclude that in these clusters, the first three H_2 molecules are bound to the three corners of the H_3^+. Structures of H_n^+, $n = 5$, 7, and 9, are shown in Fig. 1. The theory also confirms the experimental finding of Hiraoka and Kebarle[29] that the binding energies of additional H_2 molecules to H_9^+ are smaller than those of the first three H_2, as seen in Table I.

The H_5^+ ion is the transition complex for the reaction $H_3^+ + H_2$. Experiments on isotope exchange reactions have shown[37,48] that there is complete isotopic scrambling, with an activation energy of about 2.4 kcal/mol, indicating that all five H atoms can permute in the transition complex. Douglass *et al.*[49] have investigated the isotopic exchange $D_3^+ + H_2$ in reactive scattering experiments. The *ab initio* theory has found that the potential energy surface for the H_5^+ ion is very soft and shallow,[37,45,47] so that the ion easily isomerizes. Because the potential is flat near the equilibrium geometry, calculations for the dissociation energy and equilibrium geometries have not converged well. For example, Ahlrichs found the D_{2d} geometry to be the minimum, because he did not fully optimize the geometry.[37] Yamaguchi, Gaw, Remington, and Schaefer have performed impressive full CI calculations[47] with large basis sets for ten stationary points below the dissociation energy. The equilibrium geometry, shown in Fig. 1, has C_{2v} symmetry, but there are three saddle points lying less than 0.6 kcal/mol above it. Perhaps the most important is the D_{2d} structure, with the central H atom symmetrically between the two H_2. This structure is the transition state for the intramolecular proton transfer $H_3^+ \cdot H_2 \rightarrow H_2 \cdot H_3^+$ and has a barrier height of only 0.08 kcal/mol. Three of the other saddle points lie only 4.8 kcal/mol above the equilibrium geometry. The H_5^+ ion is therefore predicted to be a very nonrigid molecule.

While most calculations have focused on the structure and energetics of these ions, in 1983 Yamaguchi, Gaw, and Schaefer[45] published calculations of the harmonic vibrational frequencies of H_5^+, H_7^+, and H_9^+. They used both (DZ + P) Hartree–Fock SCF calculations for $n = 5$, 7, and 9, as well as CISD (configuration interaction, with single and double excitations) for $n = 5$ and 7. Their calculations (harmonic frequencies with an empirical scale factor) predict that the H_2 ligands in these clusters have vibrational modes with frequencies red shifted by 100 to 400 cm^{-1} from the 4161 cm^{-1} frequency of the free H_2 monomer.[50] Furthermore, they have predicted that, in H_5^+, for example, the H_3^+ moiety would absorb at approximately 3400 cm^{-1}, about 200 cm^{-1} above the predicted A_1 symmetric stretching fundamental of H_3^+. These vibrations are dipole forbidden in the respective monomers, but are predicted to become allowed in the clusters. Yamaguchi *et al.* also predict that the ν_2 (E) mode of H_3^+ at 2521 cm^{-1}, first observed by Oka[51] and subsequently the focus of much attention, is split in H_5^+ and red shifted to 1746 and 1449 cm^{-1}.

The predictions of vibrational frequencies stimulated our efforts to study the infrared spectroscopy of these cluster ions. The highest frequency modes, the H_3^+ symmetric stretch and H_2 stretching modes, are predicted to lie well above the dissociation limit for all H_n^+ clusters. Therefore, exciting the solvent H_2 will lead to cluster predissociation. In our apparatus, parent cluster ions extracted from one of a variety of sources are mass-selected and trapped. Once we have collected ions in the trap, we can excite them with a

TABLE I. Experimental and theoretical dissociation energies and enthalpies for the hydrogen cluster ions H_n^+.

Reference		5	7	9	11	13
Beuhler *et al.*[a]	ΔH^0_T	6.6 ± 0.3	3.1			
Elford[b]	ΔH^0_T	5.8 ± 1.1				
Elford and Milloy[c]	ΔH^0_T	5.8 ± 1.1				
Johnsen *et al.*[d]	ΔH^0_T	8.1 ± 0.7				
Hiraoka and Kebarle[e]	ΔH^0_T	9.6	4.1	3.8	2.4	
Bennett and Field[f]	ΔH^0_T	9.7 ± 0.2	1.8 ± 0.1			
Arifov *et al.*[g]	ΔH^0_T	5.1 ± 0.6				
Yamaguchi *et al.*[h]	$D_0(D_e)$, full CI	5.4(8.2)				
	$D_0(D_e)$, CISD	4.0(6.9)	2.6(3.4)	1.8(3.2)		
Hirao and Yamabe[i]	D_e, CISD	6.4	3.8	3.2	1.4	
	D_e, SCF	4.5	3.0	2.6	0.8	0.7
Huber[j]	D_e, SCF	5.7	3.8	3.0	1.2	1.2

[a] Reference 31.
[b] Reference 32.
[c] Reference 28.
[d] Reference 30.
[e] Reference 29.
[f] Reference 27.
[g] Reference 26.
[h] References 45 and 47.
[i] Reference 42.
[j] References 40 and 46.

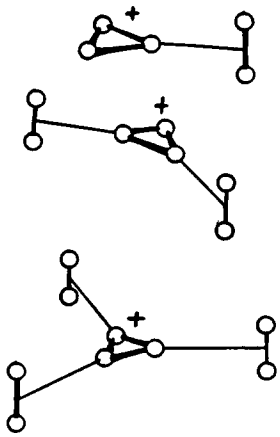

FIG. 1. Sketch of H_n^+ clusters, $n = 5$, 7, and 9, based on *ab initio* predicted geometries. See, for example, Ref. 42.

tunable infrared laser. The ion density in the trap is far too low to detect the absorption directly. Instead, we measure the absorption spectrum of the parent ion by detecting its dissociation. For weakly bound clusters, absorption of a single infrared photon by a high-frequency stretching mode can lead to predissociation of the cluster. By detecting the fragment ions produced upon dissociation as a function of laser frequency, we take advantage of the nearly unit efficiency of ion counting detection. Vibrational predissociation spectroscopy is a well known technique in the study of neutral van der Waals complexes,[52] but has had limited success with larger clusters due to both the difficulty in identifying the absorbing cluster and the uncertainties in detection stemming from cracking of the products upon electron impact ionization.

Guided by the theoretical predictions of Yamaguchi, Gaw, and Schaefer, we have searched for the H_2 stretching bands of H_n^+, $n = 5$, 7, 9, 11, 13, and 15. In addition to low-resolution observations of vibrational bands, we have sought rotationally resolved spectra, primarily of H_5^+. The light H_5^+ molecule, a near prolate symmetric top, has a rotational spacing in the P and R branches of $2B \approx 6$ cm^{-1}; therefore, one expects to observe well-resolved rotational structure, even at laser linewidths of 0.5 cm^{-1}.

II. EXPERIMENTAL

The hydrogen cluster ions were produced either by electron impact ionization of neutral H_2 clusters, or within a high pressure ($\sim$200 Torr, 0 °C) corona discharge. In the former, the ions were created with substantial amounts of excess internal energy; in the latter, the vibrational temperature of ions was expected to be near room temperature. The sources are described in more detail below. After extraction from the source, the beam of ions was mass-selected with a 20 cm radius sector magnet. The ion beam was deflected 90° in an electrostatic quadrupole bending field, decelerated to approximately 0.5 eV, then focused into a radio frequency (RF) octopole ion trap through an entrance aperture lens. Ions were collected in the trap for 0.1 to 1.0 ms; the potential of the entrance lens was then raised, and the ions confined inside the octopole.

The trap was an octopole ion guide, eight molybdenum rods 0.5 m long equally spaced on a 1.25 cm diameter circle. Details can be found elsewhere.[53] Trapped ions bounced back and forth between two lens elements, on either side of the octopole, held at a dc potential about 20 V above the trap bias. The RF on the octopole created an effective potential well perpendicular to the trap axis, confining the ions to the center of the octopole region. The pressure in this region was typically 1 to 3×10^{-9} Torr. Collisions in the trap were found to be negligible on the time scale of the experiment.

After 1 to 2 ms, an infrared laser was fired through the trap to dissociate the ions. After excitation with the laser, the ions were then released by lowering the voltage of the aperture lens at the trap exit. The ions were mass selected with a quadrupole mass spectrometer, and detected with a Daly ion detector. Standard ion counting techniques were used. In a typical experiment, counts at a given fragment ion mass were recorded as a function of laser frequency. When measuring the parent ion signal, the ion count rate was often greater than 10^6 s^{-1}. In that case, the photomultiplier gain was reduced, and the (amplified) ion current measured.

The laser was fired or chopped in alternate data cycles; the signal was the difference in fragment ion counts between cycles with the laser on and cycles with the laser off. This eliminated background fragment counts resulting from decay of metastable ions, and collision-induced dissociation in the trap. The laser power was measured after passing through the trap, for normalization of the spectra.

A. Infrared lasers

Three tunable infrared lasers were used in this experiment, covering the range from 2200 to 6500 cm^{-1}, providing a choice of average power and frequency resolution.

The optical parametric oscillator (OPO)[54] was a $LiNbO_3$ crystal pumped by the far-field output (1 W) of a Quanta Ray DCR-1A Nd:YAG laser. No line narrowing elements were in the OPO cavity; thus, the linewidth was as broad as 20 cm^{-1} (at 4200 cm^{-1}), but was more typically 5–10 cm^{-1} at the wavelengths used (3500–4000 cm^{-1}). This laser gave the highest powers, and was used for preliminary searches. The wavelength was calibrated using an 0.3 m monochromator. The laser produced 8–10 mJ per pulse at 10 Hz.

A commercial difference frequency laser was used for some moderate resolution spectra. The Quanta Ray Infrared Wavelength Extender mixes the 1.06 μm output of a Nd:YAG laser with the output of a near infrared dye laser. The laser linewidth was measured to be 1.2 cm^{-1}. The pulse energy was 0.8–1 mJ at 4000 cm^{-1} and 0.5 mJ at 3500 cm^{-1}. The laser was operated at 10 Hz.

Both of the above lasers utilize nonlinear mixing in $LiNbO_3$ crystals. This material has an unfortunate infrared absorption between 3460 and 3490 cm^{-1}. In the case of the difference frequency system, the output dropped over an order of magnitude, to 0.05 mJ per pulse or less in this range.

For high resolution experiments, spectra were taken with an F-center laser (Burleigh Instruments Inc.). Without an intracavity étalon, the laser produced 5 to 40 mW, cw, with a nominal linewidth of 0.5 cm^{-1}. With the étalon in place, the linewidth was specified as 1 MHz (3×10^{-5} cm^{-1}), far below the expected Doppler limit for trapped ions of approximately 0.08 cm^{-1}. Because this laser was con-

tinuous, the timing of the experiment was modified. When the ions were trapped, the laser beam was flagged on with a shutter (A. W. Vincent Associates) for 20 ms. As before, the laser was flagged on during alternate cycles. The low duty cycle resulted in a significant decrease in average power and signal, relative to spectra taken with the pulsed lasers. The laser wavelength was calibrated using a Burleigh λ meter.

The Doppler width of the ions was broader than a room temperature width, because the laser beam was collinear with the axis of the trap. The ions moved back and forth along this axis; for H_5^+ at a mean energy of 0.5 eV, the expected Doppler width was approximately 0.08 cm^{-1}.

B. Sources

1. Electron impact ionization of neutral $(H_2)_n$ clusters

Most of the spectra reported here were of ions produced by electron impact of neutral hydrogen clusters $(H_2)_n$. The neutral clusters were formed by supersonic expansion of pure hydrogen (99.999% pure, from Matheson or Scientific Gas Products) through a 10 μ nozzle. The stagnation conditions were 20–30 atm, at a temperature of 110 K. The expansion was skimmed with a Beam Dynamics electroformed skimmer 7 mm from the nozzle. The first region was pumped with a liquid nitrogen trapped ten inch diffusion pump backed by a 150 ℓ/s roots pump. The chamber following the skimmer was pumped by a trapped, 6 in. diffusion pump, giving a background pressure of 0.5 to 1×10^{-5} Torr. This region contained both the ionizer and electron optics. The molecular beam was ionized in a conventional hot filament electron beam ionizer. The electron energy was 80–100 eV, and the ionizer emission current was $\approx$4 mA. H_2^+ and H_3^+ were the dominant ions; the H_5^+ current was approximately 100 pA. The beam intensity decreased monotonically with cluster size, but always showed a large drop after H_9^+.

Upon ionization of the $(H_2)_n$ clusters, the reaction

$$H_2^+ + H_2 \rightarrow H_3^+ + H \qquad (1)$$

proceeds within the cluster. The excess energy in the reaction of 49 kcal/mol is deposited as internal energy in the cluster. Since, for larger clusters, the average binding energy of an H_2 is 3 kcal/mol or less,[29] the cluster probably fragments extensively. Several H_2 molecules evaporate from the cluster to carry off the excess energy.

The ionization and subsequent rearrangement and fragmentation leaves the cluster internally excited. We observed that approximately 0.1% of the ions fragment in the trap within the first 2 ms, predominantly by loss of a single H_2. The fragmentation in the trap arises from metastable ions which have survived the 50 μs flight from source to trap. Any fragments from in-flight dissociation would not have enough energy to enter the trap. Such fragmentation was not observed for ions created internally cold. Previous experiments under similar trapping conditions have shown that collisional dissociation in the trap is negligible. Thus we have direct evidence for metastable cluster ions with predissociation lifetimes on the order of milliseconds.

The background counts arising from the metastable fragmentation of H_{2n+1}^+:

$$H_{2n+1}^+ \rightarrow H_{2n-1}^+ + H_2 \qquad (2)$$

were comparable to the laser-induced dissociation signal. For spectra recorded with the H_{2n-1}^+ dissociation channel, this background was subtracted, but it consequently reduced the signal-to-noise ratio. For H_5^+, this was the only channel. The background counts were equal to the signal counts at the peak of the absorption bands, causing a significant decrease in the signal-to-noise ratio. For the larger clusters, loss of one H_2 was not a dominant dissociation channel; thus, the signal-to-noise ratio was very poor, but better spectra could be recorded using other channels involving loss of more than one H_2.

2. Corona discharge source

To eliminate spectral congestion and to reduce the background of fragment ions, a source of internally cold ions was needed. Several such sources have been described in the literature, all involving ionization at relatively high pressures ($p > 1$ Torr). There must be enough collisions for the rotational and vibrational degrees of freedom to be at least partially equilibrated with the source temperature. These sources tend to create thermodynamically stable ions,[3,55,56] often terminal ions "at the end of the food chain." Since the density of charged species is low, the presence of trace impurities can have a pronounced effect on the mass spectrum. For example, in a high pressure hydrogen discharge, the dominant ion may be H_3O^+, not H_3^+. The proton affinity of water is 165 kcal/mol,[16] 64 kcal/mol higher than that of H_2. As a result, unless the source and gas are thoroughly dried, all H_3^+ will react with trace water by very exothermic proton transfer.

Corona discharges have been used as sources of ionic clusters in a number of previous experiments.[57,58] Searcy and Fenn[59,60] developed a corona discharge source to study water cluster nucleation about an ion during a supersonic expansion, while Beuhler, Ehrenson, and Friedman[31] used one for measurements of hydrogen cluster ion equilibria prior to expansion. In the apparatus of Searcy and Fenn, a discharge was struck from a tungsten needle to a tungsten grid; the volume between the grid and a nozzle was a field-free drift region, in which the ions could equilibrate. Beuhler *et al.* did not use such a drift region. Beuhler *et al.* reported ion currents of only 10^4 ions per second; however, they used very small apertures (12 μ) to minimize cooling effects after the nozzle.

The corona discharge source used in this experiment is shown in Fig. 2. The body of the source was copper and was in thermal contact with a reservoir. It was designed for cooling with liquid nitrogen, although freon-12 and freon-22 were the primary coolants in this experiment. The electrode was a nickel-plated steel sewing needle which could be translated to vary the distance from body to point. We expected that the discharge would be located in a conical-shaped region. This tapered down at 30° to a cylindrical volume 1.0 mm in diameter, 1.7 mm in length before the nozzle in which the ions could react and equilibrate. The drift time in this region was estimated to be approximately 0.5 ms. The nozzle was a 75 μ aperture in a platinum disk (Ted Pella, Inc.). The source was floated at + 350 V above ground.

The needle was fixed at a minimum distance of 3.3 mm

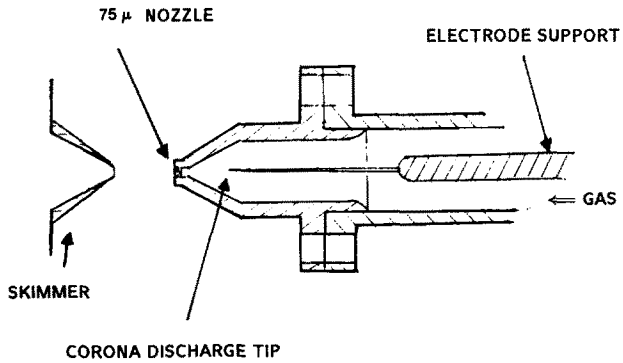

FIG. 2. Corona discharge source used to create internally cold ions. Typical source conditions were 200 Torr of H_2 at 260 K. The discharge was a positive point corona discharge with a current of 30–50 μA.

from the tapered wall of the source, 5.7 mm from the beginning of the drift region. It was in series with a 1 MΩ ballast resistor. Typical discharge conditions were 2.5 kV and 30 μA. Ultra-high-purity hydrogen (99.999% pure, as in the previous source) at 100 to 200 Torr was used. The gas was always passed through a liquid nitrogen cooled trap containing Linde 13X molecular sieve. The inlet line and the source were baked out daily and pumped to a base pressure of 10^{-5} Torr or less. Without these precautions, no hydrogen cluster ions appeared. Instead, in a "dirty" source at temperatures above approximately -10 °C, protonated water clusters were the dominant species. If the source was cooled further, the water clusters were replaced by protonated nitrogen clusters. Hydrogen cluster ions could only be produced in useful currents by keeping the source and inlet system clean.

The skimmer aperture was 1.4 mm, and was approximately 7 mm from the nozzle. The skimmer was kept to within 1 V or less of the nozzle voltage, to prevent acceleration and subsequent collisional heating of the ions. A grid surrounding this region and held at the same potential as the source was necessary to prevent stray fields from penetrating into the nozzle-skimmer region. The skimmer was followed by a conical extractor, 2 cm behind, at a potential of 10 to 20 V below the followed skimmer. Variations of this voltage could alter the ion size distribution. This result was probably due to extraction and focusing effects, because there was never any indication of collisional heating, either in the spectra or as background counts from metastable ion dissociation. The ions were then accelerated and focused. During normal operation, the pressure of the source differential chamber was 1 to 2×10^{-4} Torr, while the ion optics region after the skimmer was 6×10^{-6} Torr.

The H_5^+ current through the machine was about 3×10^5 counts/s at a source temperature of 260 K. At lower temperatures (80 K), the total ion current was comparable, but was dispersed over a large range of cluster sizes; the intensity of a given cluster was significantly lower.

III. RESULTS

A. Clusters formed by electron impact ionization

Low resolution OPO spectra were recorded from 3800 to 4200 cm^{-1} for the ions H_n^+ ($n = 5$, 7, 9, 11, 13, and 15) created by electron impact ionization. With the exception of H_5^+, all ions had a single, slightly asymmetric peak in this region. For each parent ion, we searched for spectra with the OPO at all possible fragment masses; in general, only one or two channels were important. Figure 3 shows the branching ratios of the different dissociation channels with the laser set at the peak of each absorption. In general, the major channel for each cluster was consistent with loss of the maximum number of solvent H_2 energetically allowed.

The spectrum of H_5^+, shown in the upper panel of Fig. 4 was taken with the OPO, detecting the H_3^+ fragment. The peak, at 3910 cm^{-1}, was red shifted 250 cm^{-1} from the vibrational origin of unbound H_2 monomer at 4161 cm^{-1}. In addition to an asymmetric peak, there was a long shoulder going to higher frequencies, extending over 300 cm^{-1}.

The OPO spectrum of H_7^+ is shown in the middle panel of Fig. 4. Two spectra are shown, one for dissociation to H_3^+ and one for dissociation to H_5^+. The two spectra were similar, with absorption maxima at the same frequency. The peak was more symmetric than in H_5^+, with a much smaller high-frequency shoulder. The spectrum arising from dissociation to H_3^+ was slightly broader, and had a larger relative contribution from the high-frequency shoulder. The peak occurred at 3980 cm^{-1}, with a red shift 70 cm^{-1} less than that of the H_5^+ peak.

The peak of the H_9^+ absorption at 4020 cm^{-1} shown in Fig. 4, was at an even higher frequency than those of the smaller clusters. The shift was only 40 cm^{-1} from the H_7^+ maximum. Again, spectra recorded detecting different fragments were similar, with the H_3^+ channel yielding the broadest peak, and the H_7^+ channel the narrowest. The signal-to-

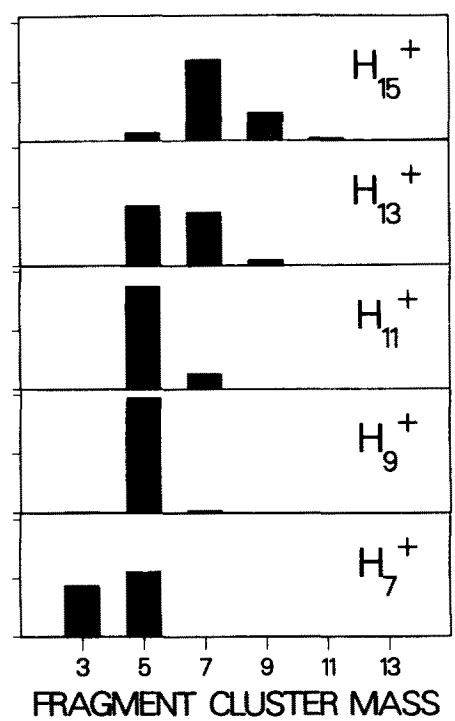

FIG. 3. Fragmentation ion branching ratios for photodissociation of H_n^+ created by electron impact ionization of neutral clusters. For each parent cluster, the laser was tuned to the absorption maximum of the H_2 stretch band.

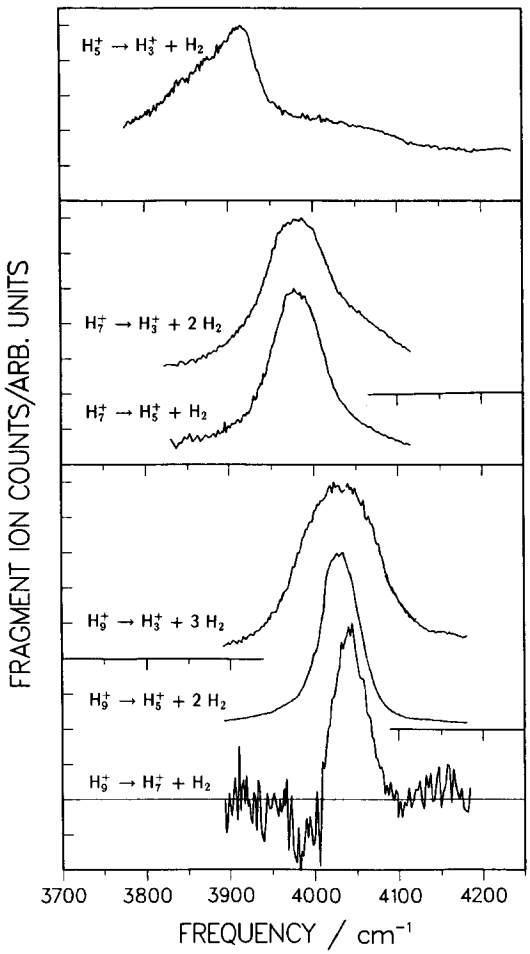

FIG. 4. Low-resolution OPO spectra of H_5^+, H_7^+, and H_9^+ (upper, middle, and lower panels, respectively). For each cluster, the spectra obtained detecting the product ions from every dissociation channel are shown. The ions were created by electron impact ionization of neutral $(H_2)_m$ clusters. Typical laser resolution ranged from 5 to 20 cm^{-1}.

noise ratio in the H_7^+ channel was low, in part because the background was higher, and in part because it was a weak channel. The dominant product by far was H_5^+, as seen in Fig. 3.

When detecting the H_7^+ fragment, an additional feature appeared in the spectrum. There was a background of H_7^+ present in the trap, created from (laser independent) dissociation in the trap of metastable H_9^+. During the laser on cycle, the laser would dissociate some of the H_7^+, giving rise to a small depletion in the background H_7^+ counts, at frequencies centered on the H_7^+ absorption at 3980 cm^{-1}. This resulted in a negative signal on the low-frequency side of the H_9^+ peak. The absolute number of background ions was small, relative to the number of parent H_9^+, and did not make a significant contribution to the signal at mass 5 or mass 3.

In the larger clusters H_{11}^+, H_{13}^+, and H_{15}^+, the peak positions at 4028, 4035, and 4048 cm^{-1} were close to that of the H_9^+ peak at 4020 cm^{-1}. Dissociation with loss of only one H_2 molecule was not observed. As seen in Fig. 3, the dominant channels were loss of three or four H_2. Only a depletion peak (as described above) was observed when detecting the channel H_{n-2}^+, peaked at the H_{n-2}^+ absorption maximum.

Spectra were recorded for all parent ions, at selected daughter ion masses, using the color center laser. The spectra shown in Fig. 5 were all taken at a resolution of 0.5 cm^{-1}, with the intracavity étalon removed. Additional scans were taken with the intracavity étalon in place, giving a laser line width of $\approx 3 \times 10^{-5}$ cm^{-1} and Doppler limited resolution of approximately 0.08 cm^{-1}. The high-resolution scans did not fully cover the peaks observed at lower resolution, but we did scan selected 5–10 cm^{-1} wide segments. We searched the H_5^+ spectrum the most intensively. In no case was any additional spectral structure resolved with the higher resolution. The signal-to-noise was worst in the high-resolution scans, usually no better than 10:1 after signal averaging. An individual scan with the intracavity étalon in place had a typical range of 0.5 cm^{-1}.

The larger clusters H_n^+, $n = 11$, 13, and 15, all exhibited a weak shoulder near 4080 cm^{-1}, which increased in relative intensity with increasing cluster size. This is seen in the OPO spectra in Fig. 6.

Based on the calculations of Yamaguchi *et al.* [45,47] we expected the mode in H_5^+ correlating to the H_3^+ symmetric stretch to occur near 3400 cm^{-1}. Figure 7 shows the peak we observed using the color center laser with 0.5 cm^{-1} resolution. It had a maximum at 3532 cm^{-1}, with an intensity approximately equal to that of the 3910 cm^{-1} peak, as predicted by Yamaguchi, Gaw, and Schaefer at the DZ + P SCF level. No rotational structure was observable at this resolution. We also scanned from 3000 to 3600 cm^{-1}, searching for the corresponding band in H_7^+ and H_9^+, but found no absorption. Any peak was therefore at least an order of magnitude less intense to go unobserved.

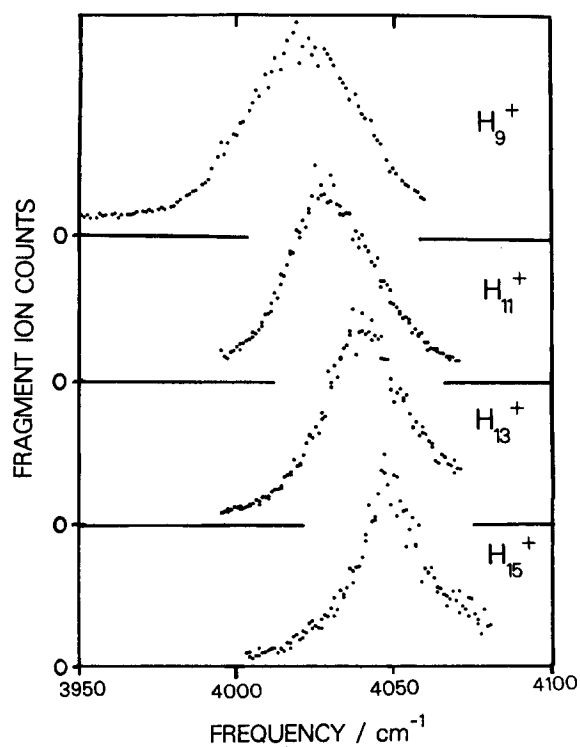

FIG. 5. Low-resolution spectra taken with *F*-center laser of (from top to bottom) H_9^+, H_{11}^+, H_{13}^+, and H_{15}^+ created by electron impact ionization.

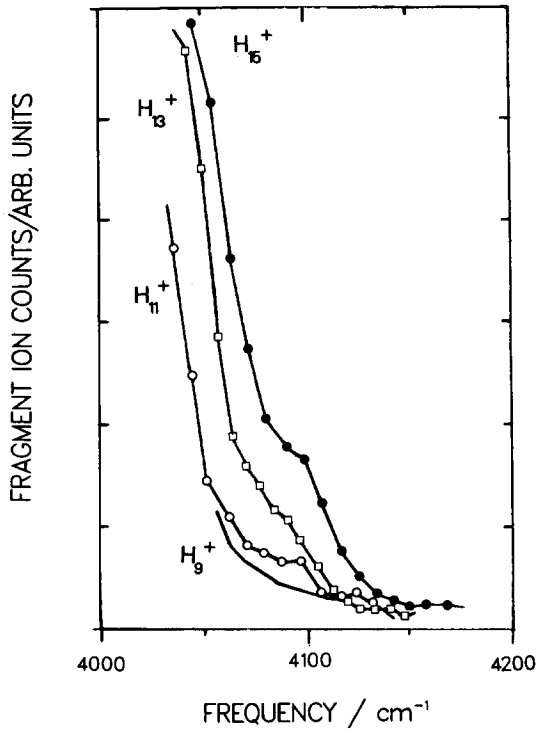

FIG. 6. Shoulder in the spectra of H_9^+, H_{11}^+, H_{13}^+, and H_{15}^+ created by electron impact ionization. All spectra were taken with the OPO at a resolution of 10 to 20 cm^{-1}, and normalized to the same peak height (full scale).

B. Results with the corona discharge source

The large fraction of metastable dissociation in the trap (up to 0.1% of the beam) indicated that clusters created by electron impact ionization had high internal temperatures. Ions extracted from the corona discharge source were expected to have vibrational temperatures at or below the source temperature (approximately -20 °C in these experiments), and rotational temperatures cooled by the supersonic expansion to well below room temperature. We expected that such cooling would considerably narrow and simplify the spectra, if they were inhomogeneously broadened. As stated above, the hydrogen cluster beam intensity of the corona discharge source was two to three orders of magnitude less intense than that of the electron impact source, and was predominantly H_5^+ at these temperatures. Thus, it was difficult to take spectra of the larger clusters. We therefore limited scans for the most part to the H_5^+ cluster.

Figure 8(b) compares the ν_1 spectrum taken with the OPO of H_5^+ formed in the corona discharge source with the spectrum of H_5^+ formed by electron impact ionization. A significant difference in the band contour was seen. The main peak at 3910 cm^{-1} did not shift, but became somewhat narrower. The high-frequency shoulder decreased in intensity, except near 4230 cm^{-1}. Thus, the spectrum of cold H_5^+ appears to have an additional weak band 320 cm^{-1} above the main band. The spectrum of H_5^+ formed by electron impact ionization could be reproduced if either the grid voltage were set to ground, or if there were a voltage drop of 10 to 30 V across the nozzle and skimmer. The difference between the two spectra is therefore caused in part by the different internal temperatures of the ions created in the two sources. Figure 9 shows the H_5^+ ν_1 spectrum taken with the difference frequency laser at a resolution of 1.2 cm^{-1}. The band has a more sharply defined peak, with a relatively flat shoulder at lower frequencies, but otherwise contains no further structure. A similar band contour was seen in the F-center spectrum of H_5^+ formed by electron impact. The detail in the lower panel [Fig. 9(b)] was taken with the WEX at 0.75 cm^{-1} resolution, and reveals the lack of structure in the spectrum.

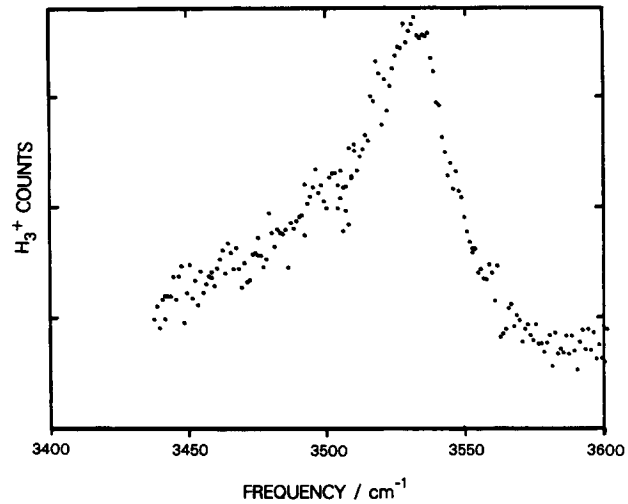

FIG. 7. Spectrum of the ν_2 mode of H_5^+, created by electron impact, taken at 0.5 cm^{-1} resolution with an F-center laser.

Again, we took extensive scans of the peak with the F-center laser, at both 0.5 and 3×10^{-5} cm^{-1} resolution, but still found no evidence of resolvable structure within the ex-

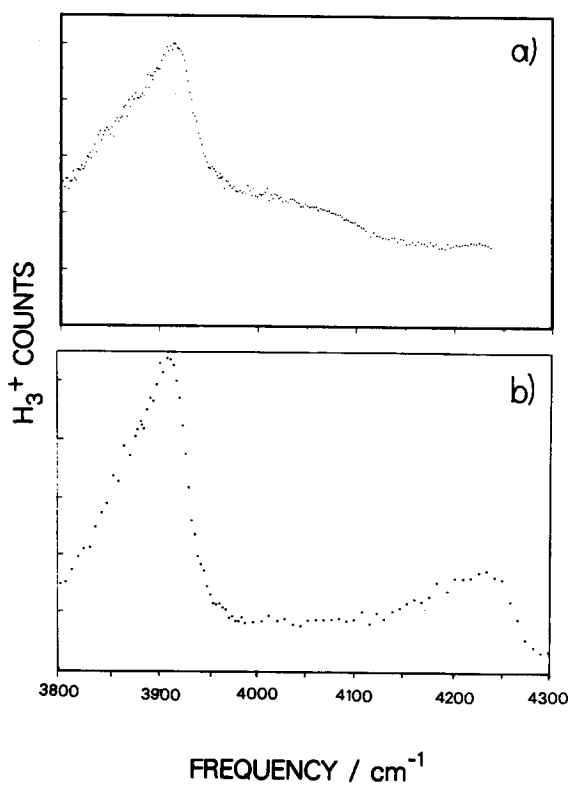

FIG. 8. Comparison of OPO spectra of H_5^+ (a) created by electron impact, and (b) created in the corona discharge source.

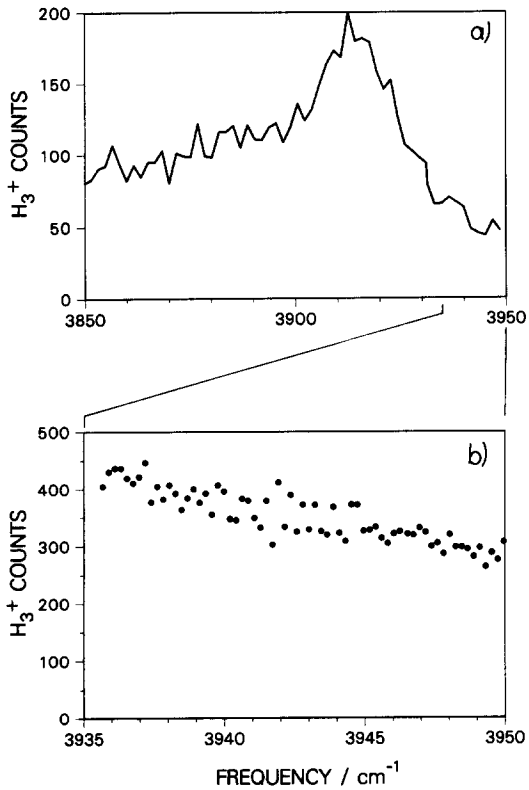

FIG. 9. (a) Spectrum of H_5^+ created in the corona discharge source, taken with the difference frequency laser and a resolution of 1.3 cm^{-1}. Lower plot shows detail of upper spectrum taken at 0.75 cm^{-1}, with higher signal-to-noise and smaller laser wavelength step size.

perimental uncertainty. We also scanned sections of the H_7^+ and H_9^+ spectra using both the *F*-center laser and the difference frequency laser, but again saw no evidence of resolvable lines.

The observation of a weak band at 4230 cm^{-1} for H_5^+ prompted a search for other weak combination bands or overtones at higher frequencies. We scanned from 3900 to 5300 cm^{-1} using the difference frequency laser (1.2 cm^{-1} resolution) in the H_5^+ spectrum, but found no new features, despite the higher laser power obtainable at these wavelengths from the difference frequency laser.

IV. DISCUSSION

A. Vibrational frequencies

The observed peak frequencies of the H_2 stretch are plotted as a function of cluster size for all observed clusters in Fig. 10. As noted above, the peaks are red shifted from the vibrational frequency of the H_2 monomer. The observed redshifts from the monomer H_2 frequency are 100 to 250 cm^{-1}, far larger than those seen in neutral H_2 complexes. In $Kr \cdot H_2$, for example,[61] the observed shift is only 1 to 2 cm^{-1}. Even in solid H_2,[62] the para $Q_1(0)$ line ($v=1, J=0$) is shifted by only 11 cm^{-1}. Bernholdt *et al.*[63] predict that the vibrational frequency of H_2 hydrogen bonded to HF will be shifted by 20 cm^{-1}. The shifts seen in H_n^+ clearly reflect the strength of the charge induced dipole interactions present in these clusters.

For H_5^+, the red shift is 250 cm^{-1}. As the cluster size increases, the frequency shift relative to the monomer frequency decreases; however, after H_9^+, the frequency shift changes very little, from 140 to 115 cm^{-1}. This result can be understood from the structures and nature of the binding predicted by the *ab initio* calculations,[37,39,45] which indicate that the H_2 molecules bind first to the three corners of the H_3^+ ion. After the first three H_2, additional H_2 molecules attach far more weakly, as depicted in Fig. 11. The reason for the lack of change in the spectrum is twofold. First, the three H_2 molecules at the corners are strongly perturbed by the ion, and thus possess the most oscillator strength at $\approx$4000 cm^{-1}. The outer H_2 molecules, darkened in Fig. 11, are far less perturbed, and thus do not absorb strongly. The weak shoulders observed near 4080–4100 cm^{-1} in clusters larger than H_9^+ may be due to absorption by these outer H_2 moieties. Second, these outer H_2 do not strongly perturb the H_9^+ core; thus, the H_2 at the corners absorb at a similar frequency, despite the added H_2 molecules.

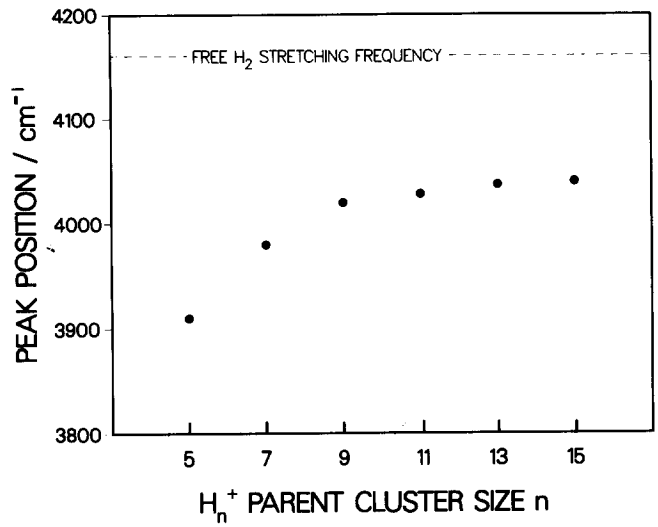

FIG. 10. Observed peak positions of the H_2 stretch as a function of cluster size.

Such a description of the larger clusters is supported by

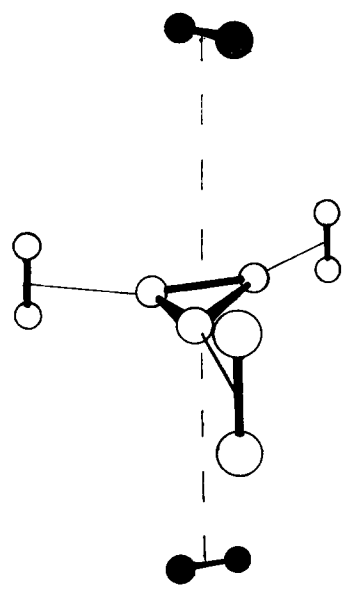

FIG. 11. Artist's conception of larger ($n>9$) hydrogen cluster ions, with the three H_2 at the corners of the H_3^+ in H_9^+ forming a complete inner solvation shell.

the trends observed in the experimental ΔH^0. Hiraoka and Kebarle have measured the enthalpies of clusters larger than H_7^+; they have found enthalpies[29] for $H_3^+ \cdot (H_2)_n \leftrightarrow H_3^+ \cdot (H_2)_{n-1} + H_2$ in H_7^+, H_9^+, and H_{11}^+ to be 4.1, 3.8, and 2.4 kcal/mol, respectively. The fourth H_2 is bound by 40% less energy than the third H_2. Their measurements for the smaller clusters disagree with the most recent experiments, implying possible systematic error, but the observed trend is probably qualitatively correct.

The location of the last two H_2 (above and below the H_3^+ plane) shown in Fig. 11 are based on SCF calculations without full geometry optimization. Such a structure does not account for the apparent stability of H_{15}^+ as seen in cluster size distributions, and collisional dissociation experiments. It might be possible to shed further light on the structure of the "second solvation" shell, if the sensitivity of the experiment were increased and details of the weaker H_2 stretches observed.

Some groups have observed the infrared absorption spectra of solid hydrogen and its isotopes after irradiation with high energy protons or β particle emission from tritium.[33–35,64] No spectra were assigned to H_n^+ entities in solid H_2 but some of the features to the red of the vibrational fundamental in the D_2 and T_2 spectra were assigned as charge-induced spectra from molecules perturbed by a positive charge. With a simple reduced mass correction, one obtains a corresponding frequency for H_2 of 4055 cm^{-1}, close to our value of 4048 cm^{-1} for H_{15}^+. The fairly large bond energies for H_9^+ formation (relative to neutral H_2 interactions), and the significant anisotropy of the potential about an H_3^+ ion suggest that H_9^+ clusters (or its isotopes) form in the solid, followed by subsequent solvation of the H_9^+. The lines observed in the solid would then be assigned to the three H_2 in the H_9^+.

Hunt and Poll[65] have calculated the Stark shift of the vibrational frequency of an H_2 molecule perturbed by a charge, as a function of the charge to H_2 separation. If one uses the *ab initio* results of Yamaguchi for an estimate of the distance between the H_2 and the H_3^+ center of charge, one obtains predicted vibrational frequencies that are 58 and 42 cm^{-1} too low for H_7^+ and H_9^+, respectively. The separation in H_5^+ is 1.855 Å, smaller than the shortest distance considered by Hunt and Poll, but extrapolation leads to an expected error of at least 60 cm^{-1}. This simple model thus appears to provide a semiquantitative estimate of the perturbed H_2 frequency, but overestimates the red shift by ~30% assuming the *ab initio* distances are correct.

Our results allow us to test the accuracy of the *ab initio* calculations of vibrational frequencies for cluster ions. Yamaguchi, Gaw, and Schaefer[45] calculated harmonic vibrational frequencies for H_n^+ using both (DZ + P basis set) Hartree–Fock SCF calculations for $n = 5$, 7, and 9, and (DZ + P basis set) single and double configuration interaction calculations (CISD) for $n = 5$ and 7. Their results, including predicted intensities, were valuable in our initial search for the spectra. Since then, Yamaguchi, Gaw, Remington, and Schaefer[47] have performed higher level theory for H_5^+, including (DZ + P) full CI as well as CI calculations with larger basis sets for several geometries. Table II lists the frequencies of the observed peak maxima for H_n^+ with $n = 5$, 7, and 9 along with the frequencies predicted by various levels of *ab initio* theory.

One must use care in comparing the experimental and theoretical vibrational frequencies. The experimental frequencies are maxima of unresolved bands, not true vibrational band origins. Bandheads and other pileups of lines could lead to band maxima displaced from the origin. This uncertainty is particularly important for H_5^+, which has an asymmetric band shape.

One of the largest uncertainties in the theoretical values lies in the scaling of frequencies to correct for both the systematic error and the anharmonicity. The calculated harmonic frequencies tend to systematically overestimate the true harmonic frequencies, as well as neglecting anharmonic effects. The theorists can crudely compensate for these errors by scaling the frequencies. Furthermore, the normal

TABLE II. Experimental and theoretical vibrational frequencies in cm^{-1} for the clusters H_n^+, $n = 5,7$, and 9. Theoretical values in parentheses are unscaled harmonic frequencies. DZ + P basis set was used for all levels tabulated here. From Refs. 45 and 47.

	Expt.[a]	Symmetry		SCF	CISD	Full CI
H_2	4161[b]			(4657)	(4533)[c]	(4515)
H_3^+	3175[d]	D_{3h}	A_1	(3604)	(3574)	(3566)
	2521[e]		E	(2905)	(2826)	(2819)
H_5^+	3910	C_{2v}	A_1	3938(4434)	3863(4235)	3844(4198)
		D_{2d}	A_1	3677(4173)	3711(4083)	3713(4067)
	3532	C_{2v}	A_1	3234(3663)	3402(3801)	3433(3824)
		D_{2d}	B_2	3659(4088)	3615(4014)	3609(4000)
H_7^+	3980	C_{2v}	A_1	3995(4491)	4008(4380)	
			B_1	3992(4488)	4004(4376)	
H_9^+	4020	C_{3v}	A_1	4020(4516)		
			E	4015(4511)		

[a] This work, except as noted.
[b] Reference 50.
[c] H_2 and H_3^+ held 1000 a_0 apart. Reference 66.
[d] Reference 67.
[e] Reference 15.

mode analysis is inadequate for weakly bound complexes with large amplitude vibrations. Recent advances[66] in the computation of anharmonic constants using analytic second derivatives should improve the accuracy of the calculations, but in cases with large anharmonic coupling, as in floppy molecules, such an expansion may not be satisfactory.

Despite the uncertainties, the theoretical and experimental values are in good agreement for H_7^+ and H_9^+. The scaled frequencies are correct to within 15 cm^{-1} at the SCF level, as seen in Table II. The agreement is more in line with previous results on strongly bound ions such as H_3O^+, and probably results from the fact that the H_2 is less strongly perturbed by the charge as the cluster size increases. Although two nearly degenerate modes are predicted for both H_7^+ and H_9^+, in each case only one band is observed.

The agreement is far worse for the H_5^+ cluster, despite the larger basis sets and use of full CI. Table II lists both harmonic and scaled vibrational frequencies, for two configurations: the C_{2v} minimum, and the low lying D_{2d} saddle point (predicted to be 0.087 kcal/mol or 30 cm^{-1} higher in energy).

For ν_1, the H_2 stretching mode observed at 3910 cm^{-1}, the DZP basis set full CI frequency is, after scaling, low by 66 cm^{-1}. Yamaguchi, Gaw, Remington, and Schaefer have calculated an "extended II" (6*s*,3*p*) basis set CISD frequency which can be scaled to obtain an estimated (6*s*,3*p*) basis set full CI frequency of 3884 cm^{-1}. This value is low by only 26 cm^{-1}. The theoretical predictions for the frequency at the saddle point geometry D_{2d} deviate the most, with an estimate 197 cm^{-1} below the observed frequency.

The ν_2 mode of H_5^+ could not be properly scaled by Yamaguchi *et al.*,[47] because the symmetric stretch of H_3^+ had not been experimentally observed. They could still estimate the scaling factor, by using a theoretical prediction for the H_3^+ symmetric stretch. This calculation involved numerically solving the vibrational Hamiltonian on a potential energy surface derived from *ab initio* points. Recently, Majewski *et al.*[67] have determined the ν_1 frequency to be 3175.0 cm^{-1} from perturbations in the ν_2 band, in excellent agreement with theoretical results.[68] This gives a scaled DZP full CI frequency of 3433 cm^{-1} for the frequency of the ν_2 mode of H_5^+ at the C_{2v} geometry, 99 cm^{-1} below our observed band at 3532 cm^{-1}. The scaled frequency at the D_{2d} geometry is 3609 cm^{-1}, 77 cm^{-1} above the observed frequency. The estimated full CI value with the extended II (6*s*,3*p*) basis set, scaled from the (6*s*,3*p*) CISD result, is 3402 cm^{-1}, 130 cm^{-1} below the observed frequency. This contrasts with the small deviation in the estimated frequency for ν_1, off by only 26 cm^{-1}, obtained at the same level of theory. We conclude that scaling *ab initio* harmonic frequencies cannot accurately predict the H_5^+ peak frequencies observed in our spectra, despite the high level of theory used.

The weak band at 4230 cm^{-1} in H_5^+ could be either a combination band or an overtone. It lies 340 cm^{-1} above the ν_1 band at 3910 cm^{-1}. Two lower frequency modes are good candidates.[45,47] Both ν_4 (H_3^+ antisymmetric stretch) and ν_8 (intermolecular stretch) modes involve large motions of the central proton, and consequently large changes in the dipole moment. These two modes are in fact the strongest absorbers of the nine vibrational modes of H_5^+, with predicted intensities in the double harmonic approximation over five and ten times larger (for ν_8 and ν_4, respectively) than the ν_1 and ν_2 modes.

The *ab initio* calculation[47] predicts that the low frequency stretch ν_8 of the complex bond has a harmonic frequency of 478 cm^{-1}. This mode is clearly anharmonic, and the true frequency is undoubtedly much lower. Thus, the weak band could be the $\nu_1 + \nu_8$ combination band. If the 4230 cm^{-1} band is assigned as the combination band $\nu_1 + \nu_8$, then the ν_8 vibrational frequency is approximately 320 cm^{-1}, neglecting the anharmonic term x_{18}. This assignment raises the question of where the $\nu_2 + \nu_8$ combination mode would lie. We predict that it would occur at 3870 cm^{-1}, only 40 cm^{-1} below the observed ν_1 band. This might give rise either to spectral congestion, or even the possibility of a Fermi resonance, since both modes will have a_1 symmetry.

The 4230 cm^{-1} band could also conceivably be an overtone. Yamaguchi, Gaw, Remington, and Schaefer predict a mode, the strong ν_4 mode, to have a harmonic frequency of 1746 cm^{-1}. Again, this number may seriously overestimate the true vibrational frequency. The scaled value for this mode is 1641 cm^{-1}, placing the second overtone at less than 4900 cm^{-1}, requiring the anharmonic term $\omega_e x_e$ to be 60 to 70 cm^{-1}.

The above discussion suggests an alternate assignment of the 3532 cm^{-1} band, as the first overtone of the 1746 cm^{-1} ν_4 mode. The intensity of the band is what one would expect, given that overtone intensities are approximately one order of magnitude weaker than the corresponding fundamentals. However, the position of the band is somewhat high; twice the calculated harmonic frequency is 3492 cm^{-1} but this is an upper bound and should severely overestimate $2\omega_e - 6\omega_e x_e$. Twice the scaled frequency is 3282 cm^{-1}, well below the observed band. Therefore, this is an unlikely candidate for the assignment of the 3532 cm^{-1} band.

B. Linewidths

Despite using high-resolution lasers, we were unable to resolve rotational structure in any of the vibrational bands. These clusters are relatively light, and from the predicted rotational constants, the rovibrational spectrum should be resolved for $n = 5$, 7, and 9. There are several possible explanations for the absence of rotational structure. The asymmetry of the peaks, particularly those of H_5^+, and the observed narrowing of the spectrum with temperature indicate that at least part of the linewidth is inhomogeneous. We can rule out instrumental artifacts, because we have observed rotational structure in the spectra of other ions created by the corona discharge source. Thus, the trapping does not give rise to unexpectedly large Doppler widths, and the instrument is in fact capable of Doppler-limited resolution.

Another possibility is that the spectrum consists of both sharp and broadened transitions. The spectrum might then appear as small lines on top of a continuous base line, and would require more signal averaging to observe the structure. From the signal-to-noise ratio in our experiment, we would conclude that the discrete spectrum must be at least ten times weaker than the continuous spectrum.

One possibility is that the spectra are very congested. The internal temperature is quite sensitive to the field between the nozzle and the skimmer; it is possible that the field was still large enough to partially heat the ions. The large rotational constants, 3.2 cm^{-1} for H_5^+ and 1.2 cm^{-1} for H_7^+, would indicate that the line density should be low; however, there are many low frequency modes which could contribute to the congestion, particularly if the molecules are internally hot. The larger clusters will also have overlapping bands at $\approx$4000 cm^{-1}, since more than one H_2 will absorb. If the H_2 stretches are coupled, they will give rise to splittings which may congest the spectra. Precedence for such congestion at or near dissociation is seen in the highly congested spectrum of H_3^+ observed by Kennedy and Carrington.[69]

The peaks could also be at least partially homogeneously broadened. This would require that the linewidth be on the order of the rotational spacing of 2 to 6 cm^{-1}. If the mechanism were lifetime broadening, the corresponding lifetimes would be approximately 1 ps. Several authors report observing such linewidths in the vibrational predissociation spectra of van der Waals complexes, e.g., the ν_7 mode of the ethylene dimer.[70,71] Attempts in other laboratories to observe H_5^+ spectra by velocity modulation absorption spectroscopy in a hydrogen glow discharge have thus far failed.[72] This high resolution technique cannot detect significantly broadened transitions. The inability to detect any transitions can be explained if the transitions have large, homogeneously broadened linewidths. However, the high vibrational temperatures and low pressures may limit the concentration of H_5^+ in the discharge, and the negative result is therefore not conclusive.

The clusters H_7^+ and larger, as well as their products after loss of one H_2, possess several low frequency vibrations and internal rotations. Therefore, these clusters will have very high densities of states at 4000 cm^{-1}. Furthermore, there will be many rovibrational dissociation channels available. The interaction between an H_2 at the corner of the H_3^+ and the H_3^+ is very anisotropic, so dissociation leading to loss of an H_2 occupying a corner site can proceed with transfer of excess energy into rotation.[70,73] The small moments of inertia of H_2 and H_3^+ allow large energy transfer to rotation with very small changes in rotational quantum numbers. For these reasons, one might expect these clusters to undergo efficient vibrational predissociation.

C. The H_5^+ ion

The recent calculations of Yamaguchi *et al.*[47] have begun to give us a clearer picture of the H_5^+ ion. Their high level *ab initio* calculations have found the H_5^+ potential to be very flat. The resulting difficulty in pinpointing the exact location of the equilibrium geometry has prompted theorists[37,39,42,45,47] to conclude that among the hydrogen cluster ions, the H_5^+ ion deviates the most from the simple model of an H_2 molecule weakly bound to an H_3^+ ion. In this section, we examine what is known of the H_5^+ potential energy surface, and discuss implications for the vibrational frequencies and dynamics.

Considered as $H_2 \cdots H^+ \cdots H_2$, it is the simplest of the proton bound complexes $A \cdots H^+ \cdots B$ such as $H_3O^+ \cdot H_2O$, $NH_4^+ \cdot NH_3$, and $H_3O^+ \cdot NH_3$. Theorists[42,74] have investigated these complexes extensively. Experimental studies in the gas phase are far more limited. The location of the proton depends to a first approximation on the relative proton affinities of the two bases. At small separations, the potential well for the proton tends to be very flat; as the bases are pulled apart, the potential bifurcates and becomes a double minima well. At the equilibrium separation, the nature of the well, single or double, depends on the pair of bases A and B. In neutral hydrogen-bonded dimers such as $(HF)_2$ and $(NH_3)_2$, there is no question of proton transfer. The vibrational problem of intramolecular proton transfer is well known,[75,76] but has not been solved quantitatively for an isolated complex.

In their extensive study of H_5^+, Yamaguchi, Gaw, Remington, and Schaefer have computed the properties of ten stationary points at very high levels of theory, and found only one minimum. Their calculations show that there are three saddle points lying less than 0.6 kcal/mol above the energy minimum. These differences are in fact at the limit of the accuracy of these calculations. The minimum energy geometry is the C_{2v} $H_3^+ \cdot H_2$, but the D_{2d} transition state for intramolecular proton transfer to $H_2 \cdot H_3^+$ is calculated to be only 0.08 kcal/mol or 30 cm^{-1} higher at the full CI level using an extended (larger than DZ + P) basis set. The calculated harmonic frequency is 478 cm^{-1} at the (DZ + P) full CI level. Thus, the D_{2d} barrier lies below the zero-point energy level, and the zero-point motion therefore involves the isomerization $H_3^+ \cdot H_2 \rightleftharpoons H_2 \cdot H_3^+$. The height of the barrier depends upon the separation between the two H_2. As the intermolecular distance between the two H_2 is stretched, the barrier height will increase, and the proton, finding itself in a double well, must follow one of the H_2. The proton transfer well thus adiabatically changes as the complex undergoes low-frequency stretching.

Another low-frequency motion is the torsional mode. This is the propeller-like rotation of the H_2 molecule about the C_2 axis. The C_{2v} barrier for this internal rotation at the extended basis set full CI level is only 128 cm^{-1}. At most, only two rotational levels could lie below this barrier. Thus, the internal rotation is only slightly hindered.

The third low lying stationary point, with D_{2h} symmetry, is the planar barrier for H_2 rotation from the symmetric D_{2d} configuration. The energy of this point is 178 cm^{-1}, very nearly the sum of the two previous barrier heights. Thus, the barrier for internal rotation is very low, regardless of the location of the central proton.

The in-plane rotation of the H_3^+ about its own C_3 top axis has a much larger barrier, calculated by Yamaguchi *et al.* to be 4.8 kcal/mol (DZ + P full CI). It is readily seen that combinations of the above isomerizations can lead to exchange of any pair of hydrogen atoms in H_5^+. Thus, compared to a rigid structure, all five H atoms can be permuted, and the floppy H_5^+ can access $5! = 120$ C_{2v} potential minima. The large amplitude motions greatly increase the number of states, relative to a naive, rigid molecule assumption. This may result in a more congested spectrum than expected, as well as a significantly larger density of states at the

dissociation energy. However, nuclear spin symmetry considerations for such high permutational symmetry greatly reduce the expected degeneracy and splittings.

What are the vibrational modes of such a nonrigid molecule? Can normal mode analysis properly predict the vibrational frequencies? As seen in Table II, both the ν_1 and ν_2 vibrational frequencies change by over 200 cm^{-1} from the C_{2v} geometry to the D_{2d} geometry, and they become nearly degenerate. The ν_3 through ν_5 modes, which involve stretching of the bonds being formed/broken, change by 200 to 400 cm^{-1}, while the other three modes are relatively unchanged. The observed frequencies should not be interpreted as a means of choosing between two alternate equilibrium geometries. The large changes in vibrational frequencies with small changes in the stretching of the weak bond imply coupling of these higher vibrations with this low-frequency coordinate (labeled ν_8 in the C_{2v} geometry). The empirical scaling of the harmonic frequencies should only account for the anharmonicity inherent in the isolated molecule. The anharmonic mixing of modes may be so strong that the harmonic frequencies predicted from the equilibrium geometry would be of limited use.

Examination of the *ab initio* calculations suggest that the coordinate associated with the 478 cm^{-1} mode changes in character from an intermolecular stretch at large separations, to purely motion of the central proton at the saddle point. In other words, the intermolecular stretch, i.e., the dissociation coordinate, is strongly coupled to the proton motion, and in turn to the higher frequency modes in H_5^+. This picture is consistent with the large change in vibrational frequencies for those normal modes such as the H_3^+ antisymmetric stretches which include motion of the central H.

It is not clear that a Taylor expansion of the potential at the equilibrium geometry alone will adequately represent the full potential surface. The anharmonic interactions may be too large. At the least, a numerical solution of the dynamics of the two large amplitude degrees, the stretching of the $H_3^+ \cdots H_2$ bond and the central proton transfer motion, seems necessary to accurately predict the vibrational frequencies and splittings in H_5^+. The ν_3 and ν_4 modes should be particularly sensitive to the accuracy of the dynamical calculation. The ν_4 mode is predicted to have a large intensity, and a better estimate of its frequency would greatly aid the search for this band in direct absorption experiments.

The large couplings in H_5^+ may also explain the observed linewidths. In general, vibrational predissociation of complex clusters is not yet fully understood.[52] As mentioned in the previous section, the large rotational constants of the products, and the relatively high density of states should facilitate predissociation of H_5^+ excited 1500 to 2000 cm^{-1} above the dissociation limit. The discussion here suggests that rapid dissociation may also be a consequence of the strong coupling between the H_2 stretches, the proton motion, and the dissociation coordinate. With four electrons, calculation of at least part of the H_5^+ potential energy surface should be practical. Studies of the dynamics on this surface should yield insights into the problems of intramolecular proton transfer, cluster vibrations, and cluster predissociation.

V. SUMMARY

Using vibrational predissociation spectroscopy, we have observed the H_2 stretching vibration in the infrared spectra of the ionic clusters H_n^+, with $n = 5, 7, 9, 11, 13$, and 15. We have also observed the H_3^+ symmetric stretch mode in H_5^+. These spectra are an important first step in our investigation of the infrared spectroscopy of cluster ions. The H_2 stretch band positions we have observed for these clusters are consistent with the prediction that H_5^+ is a stable species, with a completed coordination shell of three H_2 at each corner of the H_3^+ ion. Spectra of all ions were scanned at 0.5 cm^{-1} resolution, but in no case were rovibrational lines observed. The spectrum of H_5^+ was searched at Doppler limited resolution (<0.08 cm^{-1}), but again no resolvable lines were seen, although the expected line spacing was 6 cm^{-1}. To eliminate hot bands and congestion, the ions were created in a high-pressure corona discharge source to create thermalized ions. Only a change in the band contour was observed, including the emergence of a weak combination or overtone band. These results indicate the possibility of homogeneous broadening. Calculations by *ab initio* theory suggest that H_5^+ has a very shallow potential surface. We have discussed possible implications, based on the theoretical information available. Calculations of the H_5^+ potential energy surface and dynamics are eagerly awaited. Most of the effort reported in this paper was expended searching the H_5^+ spectrum. Selected high resolution scans of the spectra of the larger clusters H_7^+ and H_9^+ also revealed no structure, but the scans covered only a limited range. No scans using the *F*-center laser or the difference frequency laser were performed for the larger clusters created in the discharge source. A more detailed examination of the larger clusters therefore would be in order. It might also be interesting to search for weak absorption by the outer H_2 molecules in the larger clusters.

A clear extension of this work would be to study the deuterated isotopes of H_5^+. More exotic hydrogen clusters can also be studied. Even mass clusters H_4^+, H_6^+, and H_8^+ have been observed in a mass spectrometer by Kirchner, Gilbert, and Bowers.[77] Theoretical work suggests that the geometry of the H_4^+ is $H_3^+ \cdots H$, with a dissociation energy comparable to that of H_5^+. Such an ion should have a symmetric H_3^+ stretch mode at approximately 3500 cm^{-1}, similar to that of H_5^+. The negatively charged hydrogen cluster ions would also be worth studying. Recent calculations[41,42] indicate that they are bound with energies roughly an order of magnitude less than the positive clusters H_n^+, and their structures are quite different: The H_2 are solvated around a single H^-, and thus the octahedral H_{13}^- is predicted to be the ion with the completed inner shell.

ACKNOWLEDGMENTS

We would like to thank Y. Yamaguchi, J. F. Gaw, and H. F. Schaefer for many stimulating discussions, and for providing us with the results of their calculations prior to publication. This work was suppported by the Director, Office of Energy Research, Office of Basic Energy Sciences,

Chemical Sciences Division of the U.S. Department of Energy under Contract No. DE-AC-0376SF00098.

[1] E. E. Ferguson, F. C. Fehsenfeld, and D. L. Albritton, in *Gas Phase Ion Chemistry*, edited by M. T. Bowers (Academic, New York, 1979), Vol. I.
[2] T. D. Mark and A. W. Castleman, Adv. At. Mol. Phys. **20**, 65 (1985).
[3] P. Kebarle, Annu. Rev. Phys. Chem. **28**, 445 (1977).
[4] A. W. Castleman and R. G. Keesee, Chem. Rev. **86**, 589 (1986).
[5] T. A. Miller and V. E. Bondeybey, *Molecular Ions: Spectroscopy, Structure, and Chemistry* (North-Holland, Amsterdam, 1983).
[6] R. J. Saykally and C. S. Gudeman, Annu. Rev. Phys. Chem. **35**, 387 (1984).
[7] R. A. Kennedy and T. A. Miller, J. Chem. Phys. **85**, 2326 (1986).
[8] P. J. Brucat, L.-S. Zhang, C. L. Pettiette, S. Yang, and R. E. Smalley, J. Chem. Phys. **84**, 3078 (1986).
[9] J. V. Coe, J. T. Snodgrass, C. B. Freidhoff, K. M. McHugh, and K. H. Bowen, J. Chem. Phys. **83**, 3169 (1985).
[10] J. V. Coe, J. T. Snodgrass, C. B. Freidhoff, K. M. McHugh, and K. H. Bowen, Chem. Phys. Lett. **124**, 274 (1986).
[11] L. A. Posey, M. J. DeLuca, and M. A. Johnson, Chem. Phys. Lett. **131**, 170 (1986).
[12] M. Bogey, H. Bolvin, C. Demuynk, and J. L. Destombes, Phys. Rev. Lett. **58**, 988 (1987).
[13] M. Okumura, L. I. Yeh, and Y. T. Lee, J. Chem. Phys. **83**, 3705 (1985).
[14] M. Okumura L. I. Yeh, J. D. Myers and Y. T. Lee J. Chem. Phys. **85**, 2328 (1986).
[15] T. Oka, in *Molecular Ions: Spectroscopy, Structure, and Chemistry*, edited by T. A. Miller and V. E. Bondeybey (North-Holland, Amsterdam, 1983).
[16] S. G. Lias, J. F. Liebman, and R. D. Levin, J. Phys. Chem. Ref. Data **13**, 695 (1984).
[17] P. H. Dawson and A. W. Tickner, J. Chem. Phys. **37**, 672 (1962).
[18] K. Buchheit and W. Henkes, Z. Angew. Phys. **24**, 191 (1968).
[19] R. Clampitt and L. Gowland, Nature **223**, 816 (1969).
[20] S. L. Anderson, T. Hirooka, P. W. Tiedemann, B. H. Mahan, and Y. T. Lee, J. Chem. Phys. **73**, 4779 (1980).
[21] A. van Deursen, A. van Lumig, and J. Reuss, Int. J. Mass Spectrom. Ion Phys. **18**, 129 (1975).
[22] A. van Lumig and J. Reuss, Int. J. Mass Spectrom. Ion Phys. **25**, 137 (1977).
[23] A. van Lumig and J. Reuss, Int. J. Mass Spectrom. Ion Phys. **27**, 1197 (1978).
[24] A. van Lumig, J. Reuss, A. Ding, J. Weise, and A. Rindtisch, Mol. Phys. **38**, 337 (1978).
[25] N. J. Kirchner and M. T. Bowers, J. Phys. Chem. **91**, 2573 (1987).
[26] U. A. Arifov, S. L. Pozharov, I. G. Chernov, and Z. A. Mukhamediev, High Energy Chem. (U.S.S.R.) **5**, 69,79 (1971).
[27] S. L. Bennett and F. H. Field, J. Am. Chem. Soc. **94**, 8669 (1972).
[28] M. T. Elford and H. B. Milloy, Aust. J. Phys. **27**, 211, 795 (1974).
[29] K. Hiraoka and P. Kebarle, J. Chem. Phys. **62**, 2267 (1975).
[30] R. Johnsen, C. M. Huang, and M. A. Biondi, J. Chem. Phys. **65**, 1539 (1976).
[31] R. J. Beuhler, S. Ehrenson, and L. Friedman, J. Chem. Phys. **79**, 5982 (1983).
[32] M. T. Elford, J. Chem. Phys. **79**, 5951 (1983).
[33] R. L. Brooks, J. L. Hunt, J. R. MacDonald, J. D. Poll, and J. C. Waddington, Can. J. Phys. **63**, 937 (1985).
[34] R. L. Brooks, M. A. Selen, J. L. Hunt, J. R. MacDonald, J. D. Poll, and J. C.Waddington, Phys. Rev. Lett. **51**, 1077 (1983).
[35] P. C. Souers, E. M. Fearon, P. E. Roberts, R. T. Tsugawa, J. D. Poll, and J. L. Hunt, Phys. Lett. A **77**, 277 (1989).
[36] R. A. Poshusta and F. A. Matsen, J. Chem. Phys. **47**, 4795 (1967).
[37] R. Ahlrichs, Theor. Chim. Acta **39**, 149 (1975).
[38] W. I. Salmon and R. D. Poshusta, J. Chem. Phys. **59**, 4867 (1973).
[39] S. Yamabe, K. Hirao, and K. Kitaura, Chem. Phys. Lett. **56**, 546 (1978).
[40] H. Huber, Chem. Phys. Lett. **70**, 353 (1980).
[41] L. R. Wright and R. F. Borkman, J. Chem. Phys. **77**, 1938 (1982).
[42] K. Hirao and S. Yamabe, Chem. Phys. **80**, 237 (1983).
[43] H. Huber and D. Szekely, Theor. Chim. Acta **62**, 499 (1983).
[44] S. Raynor and D. R. Hershbach, J. Phys. Chem. **87**, 289 (1983).
[45] Y. Yamaguchi, J. Gaw, and H. F. Schaefer III, J. Chem. Phys. **78**, 4074 (1983).
[46] H. Huber, J. Mol. Struct. **121**, 281 (1985).
[47] Y. Yamaguchi, J. F. Gaw, R. B. Remington, and H. F. Schaefer III, J. Chem. Phys. **86**, 5072 (1987).
[48] V. L. Talrose, P. S. Vinogradov, and I. K. Larin, in *Gas Phase Ion Chemistry*, edited by M. T Bowers (Academic, New York, 1979).
[49] C. H. Douglass, G. Ringer, and W. R. Gentry, J. Chem. Phys. **76**, 2423 (1982).
[50] K. P. Huber and G. Herzberg, *Molecular Spectra and Molecular Structure: IV. Constants of Diatomic Molecules* (Van Nostrand Reinhold, New York, 1979).
[51] T. Oka, Phys. Rev. Lett. **45**, 531 (1980).
[52] R. E. Miller, J. Phys. Chem. **90**, 3301 (1986).
[53] S. W. Bustamente, M. Okumura, D. Gerlich, L. R. Carlson, H. S. Kwok, and Y. T. Lee, J. Chem. Phys. **86**, 508 (1987).
[54] S. J. Brosnan and R. L. Byer, IEEE J. Quantum Electron **15**, 415 (1979).
[55] K. R. Jennings, in *Gas Phase Ion Chemistry*, edited by M. T Bowers (Academic, New York, 1979), Vol. 20.
[56] M. W. Siegel and W. L. Fite, J. Phys. Chem. **80**, 2871 (1976).
[57] H. Kambara and I. Kanomata, Anal. Chem. **49**, 270 (1977).
[58] V. J. Caldecourt, D. Zakett, and J. C. Tou, Int. J. Mass Spectrom. Ion Phys. **49**, 233 (1983).
[59] J. Q. Searcy and J. B. Fenn, J. Chem. Phys. **61**, 5282 (1974).
[60] J. Q. Searcy, J. Chem. Phys. **63**, 411 (1975).
[61] A. R. W. McKellar, Faraday Discuss. Chem. Soc. **73**, 89 (1982).
[62] S. A. Boggs, M. J. Clouter, and H. L. Welsh, Can. J. Phys. **59**, 2064 (1972).
[63] D. E. Bernholdt, S. Liu, and C. E. Dykstra, J. Chem. Phys. **85**, 5120 (1986).
[64] P. C. Souers, E. M. Fearon, R. L. Stark, R. T. Tsugawa, J. D. Poll, and J. L. Hunt, Can. J. Phys. **59**, 1408 (1981).
[65] J. L. Hunt and J. D. Poll, Can. J. Phys. **63**, 84 (1985).
[66] Y. Yamaguchi and H. F. Schaefer III (private communication).
[67] W. A. Majewski, M. D. Marshall, A. R. W. McKellar, J. W. C. Johns, and J. K.G. Watson, J. Mol. Spectrosc. **122**, 341 (1987).
[68] W. Meyer, P. Botschwina, and P. Burton, J. Chem. Phys. **84**, 891 (1986).
[69] A. Carrington and R. A. Kennedy, J. Chem. Phys. **81**, 91 (1984).
[70] W. R. Gentry, ACS Symp. Ser. **263**, 289 (1984).
[71] A. Mitchell, M. J. McAuliffe, C. F. Giese, and W. R. Gentry, J. Chem. Phys. **83**, 4271 (1985).
[72] J. Owrutsky and R. J. Saykally (private communication).
[73] G. Ewing, Faraday Discuss. Chem Soc. **73**, 325 (1982).
[74] S. Scheiner, Acc. Chem. Res. **18**, 174 (1985).
[75] P. Schuster, G. Zundel, and C. Sandorfy, *The Hydrogen Bond. Recent Developments in Theory and Experiments* (North-Holland, Amsterdam, 1976), Vols. 1–3.
[76] T. Carrington, Jr. and W. H. Miller, J. Chem. Phys. **84**, 4364 (1986).
[77] N. J. Kirchner, J. R. Gilbert, and M. T. Bowers, Chem. Phys. Lett. **102**, 7 (1984).